Available online at www.sciencedirect.com

SciVerse ScienceDirect

Ceramics International 38 (2012) 1077–1083

CERAMICS INTERNATIONAL

www.elsevier.com/locate/ceramint

Effect of composition and annealing on the dielectric properties of ZnO/mullite composite coatings

Liang Zhou *, Wancheng Zhou, Jinbu Su, Fa Luo, Dongmei Zhu

State Key Laboratory of Solidification Processing, Northwestern Polytechnical University, Xi'an 710072, China

Received 15 August 2011; accepted 15 August 2011
Available online 24 August 2011

Abstract

ZnO/mullite composite coatings were fabricated by atmosphere plasma spraying technology (APS). Scanning electron microscopy (SEM) and X-ray diffraction (XRD) were employed to investigate the microstructures and compositions of the feedstock and coatings. The permittivity–frequency properties were determined in the microwave frequency range of 8.2–12.4 GHz by network analysis. Our results show that both the real and imaginary part of permittivity increase greatly with increasing ZnO content over the frequency range of 8.2–12.4 GHz, which can be ascribed to interfacial polarization and orientation polarization. However, the composite coatings after 900 °C annealing for 5 h show much lower permittivity, due to the decrease of ZnO content resulting from the further reactions between the ZnO and mullite. Results indicate that the composite coating has excellent permittivity in room temperature, while for high temperature application, more investigation should be done.

Keywords: C. Dielectric properties; Plasma spraying; Radar absorbing coating; ZnO/mullite composite coatings

1. Introduction

Plasma spraying is a well-known industrial technique, suitable to make metallic or ceramic coatings [1]. Oxide ceramic coatings are used to improve the resistance to corrosion, heat and wear of metal component. Mullite ($3Al_2O_3{\cdot}2SiO_2$) is an important engineering ceramic, featuring excellent high-temperature strength, low thermal conductivity, favorable creep behavior and chemical stability at temperatures as high as 1500 °C [2–5]. Thus, mullite-based ceramic coatings are being developed as thermal barrier coatings for application in space [6]. These composite coatings cover a wide range of materials including: mullite/ZrO_2 [7,8], mullite/Al_2O_3 [9], mullite/SiC [10], and mullite/Mo [11].

Recently, with the progresses in the utilization of electrical and electronic devices, radar-absorbing coatings have attracted considerable attention in commercial and military applications [12,13]. Because of the wide direct-band gap of 3.3 eV as a II–VI compound semiconductor, ZnO has attracted much attention as a new and promising electromagnetic wave-absorbing material. Oku et al. [14] prepared ZnO/polymer composite that can absorb and shield electromagnetic waves and eliminate static charge deposition in some electron devices. Dang et al. [15] investigated the dielectric properties of polyethylene composites filled with whisker and nanosized zinc oxide.

Composite materials, consisting of insulating matrix dispersed electrical conductive fillers, are usually used to fabricate composite coatings in radar absorbing applications [16,17]. The electrical characteristics of such composite coatings are close to the properties of the fillers, whereas their mechanical properties and processing methods are typical for insulating matrix. In the present paper, the ZnO/mullite composite absorbing coatings were deposited by atmosphere plasma spraying (APS) technique. The microstructure and the microwave absorbing of the coating and powders were tested. And the permittivity–frequency properties were determined in the microwave frequency range of 8.2–12.4 GHz by network analysis.

2. Experimental

2.1. Preparation of the powder

Commercial ZnO powder (≥99.0 wt.%; D50 = 9 μm) and mullite powder (>99.9 wt.%; D50 = 0.8 μm) were used as

* Corresponding author. Tel.: +86 029 88494574; fax: +86 029 88494574.
E-mail address: zhouliang83@163.com (L. Zhou).

0272-8842/$36.00.
doi:10.1016/j.ceramint.2011.08.034

Table 1
Formulation of the slurry used for the spray-drying.

Components	Quantity
Solid particles: ZnO/mullite composite powders	50 wt.%
Dispersant: tetraethyl ammonium hydroxide	0.2 wt.%
Binder: poly vinyl alcohol (PVA)	3.0 wt.%

Table 2
Spray-drying operating conditions.

Entry air temperature (°C)	280–300
Chamber air temperature (°C)	180
Exit air temperature (°C)	120–130
Rotational speed of nozzle (rpm)	32,000
Slurry feed rate (g/min)	100
Atomizing air flow rate (m^3/h)	20

starting raw materials. ZnO and mullite powders were taken in the weight ratios of 40/60, 50/50, 60/40, 70/30 and 80/20 and agglomerated using spray-drying technology.

In the spray-drying technique, both the slurry properties and drying conditions affect the spray-dried particles [18]. In order to achieve self-standing ceramic powders by spray-drying technology, the suspension must contain high concentration of solid materials and be stable during the process. The composition of slurry with ZnO/mullite composite powders is shown in Table 1.

The main controlled spray parameters are the air temperature, rotational speed of nozzle, slurry feed rate and atomizing air flow rate. The conditions used in this study are listed in Table 2. The ambient air temperature was achieved in the spray dryer chamber leading to a rapid evaporation of the liquid phase.

2.2. Preparation of the coating

Low power plasma spray system with an internally fed powder torch was used in this study. A schematic diagram of the plasma spray equipment is shown in Fig. 1. It consists of a DC electrical power source, gas flow control, water-cooling system and powder feeder. The electric arc discharge, supported by the DC electrical power source heats up the plasma gases, which expand in the atmosphere, forming a jet. The powder, suspending in the carrier gas, is injected into the jet. After being melted and accelerated in the jet, the particles impact the work piece and form the coating.

The coatings were prepared by the low power plasma spraying system described above with Ar and N_2 as plasma gases at a flow rate of 14 and 2 standard liters per minute (slpm), respectively. More details about the spraying parameters are reported in Table 3. The coatings were sprayed about 3.5 mm in thickness on graphite substrates. After deposition, they were mechanically removed from the substrates.

2.3. Characterizations of powders and coating

The phases of both the feedstock and the coatings were identified by X-Ray diffraction (D/MAX2500 diffractmeter) with Cu-Kα radiation. The scanning electronic microscope (JEOL JSM-6360LV) was used to reveal the microstructure of the feedstock and the coatings.

The testing specimens were cut into rectangular blocks with dimensions of 10.16 mm (width) × 22.86 mm (length) × 2 mm (thickness) for the measurement of dielectric properties. The dielectric parameters were determined by E8362B PNA network analyzer with wave guide method in the frequency range of 8.2–12.4 GHz.

3. Results and discussion

3.1. Microstructure and phase composition of powders

Fig. 2(a) shows the SEM micrograph of the spray-dried particles. It could be found that the particles are spherical shape,

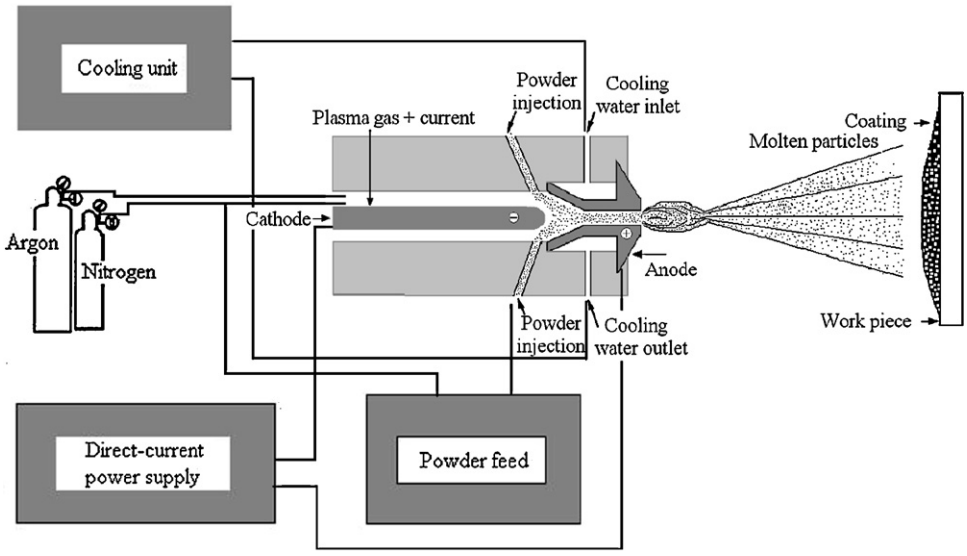

Fig. 1. Schematic diagram of low power spray system.

Table 3
Plasma spraying parameters.

Parameters	Value
Arc current (A)	240
Arc voltage (V)	35
Primary gas ($Ar + N_2$) flow rate (slpm)	14
Secondary gas (N_2) flow rate (slpm)	2
Spray distance (mm)	100
Powder carrier gas flow rate (slpm)	4
Powder feed rate (g/min)	3

and the particle size ranges from 40 to 90 μm. Fig. 2(b) shows the XRD pattern of the prepared ZnO/mullite composite particles. It can be confirmed that the diffraction peaks corresponding to both ZnO and mullite can be seen clearly, and there are no other diffraction peaks except ZnO and mullite.

3.2. Microstructure and crystalline phase of coatings

A thermal spray coating is produced by the deposition of numerous consequent layers formed by flattening and solidification of molten or partially molten particles impinging at high velocity on the substrate or on previously deposited layers. Fig. 3(a)–(f) are cross-sectional SEM morphologies of the as-sprayed ZnO/mullite composite coating. In all the coatings, elongated splats form a curved lamellar structure, as indicated by arrows, which is typical of spray coatings. Further more, all the coatings show a dense structure with a few pores. And the white and gray areas indicate mullite and zinc oxide, respectively. The porosity increased with raising the amount of ZnO ceramics. This is likely due to an incomplete melting of the ZnO ceramics during deposition since the mullite are easily melted and coated on the substrate. The coatings with lower ZnO content (Fig. 3(a) and (b)) shows litter lamellar structure and partly melted ZnO particles with larger particle size impinging on the $ZnAl_2O_4$, Zn_2SiO_4 and mullite matrix. On the other hand, the coatings with 60 and 70 wt.% ZnO content (Fig. 3(c) and (d)) show a different structure from the coatings shown in Fig. 3(a) and (b), which is probably due to the less $ZnAl_2O_4$, Zn_2SiO_4 and mullite content. However, there are many unmelted powders and pores in the coating with 80 wt.% ZnO content as shown in Fig. 3(e). And the inclusions of unmelted ZnO particles between the splats were observed locally as a result of a partial melting with spraying.

The XRD pattern of the as-sprayed composite coatings is shown in Fig. 4. It can be seen that all the coatings are composed of ZnO, $3Al_2O_3{\cdot}2SiO_2$, $ZnAl_2O_4$ and Zn_2SiO_4. The absence of $ZnAl_2O_4$ and Zn_2SiO_4 indicates that the ZnO-mullite system is incompatible at the high temperature (plasma spraying condition). In fact, this is in agreement with the phase diagram of $ZnO–Al_2O_3–SiO_2$ system reported by Bunting [19]. According to the isothermal section at 1700 °C, there is a three-phase compatible section that involves species $ZnAl_2O_4$, Zn_2SiO_4 and $3Al_2O_3{\cdot}2SiO_2$. During the process of plasma spraying, the following reactions between $3Al_2O_3{\cdot}2SiO_2$ and ZnO, involving the decomposition of $3Al_2O_3{\cdot}2SiO_2$, are proposed:

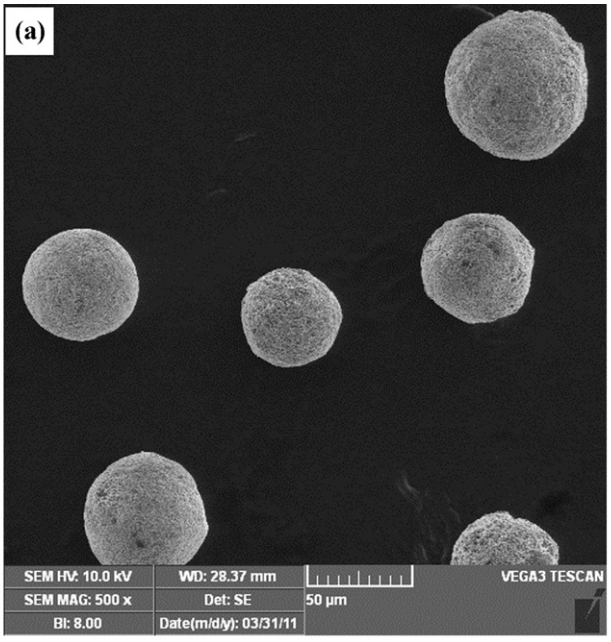

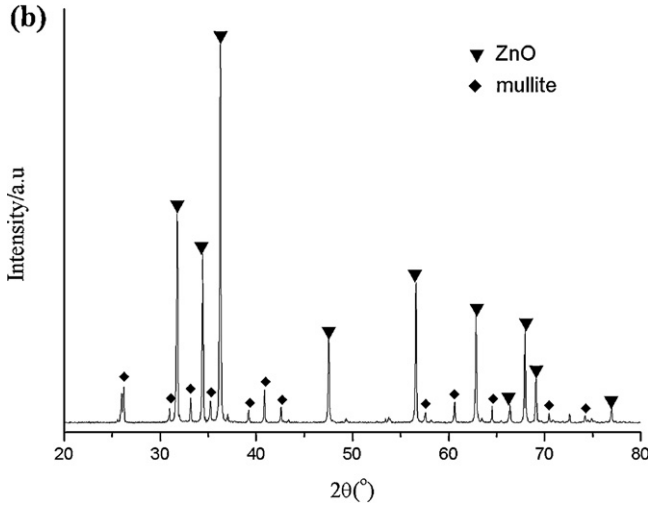

Fig. 2. (a) SEM micrograph and (b) X-ray diffraction of the spray-dried ZnO/mullite composite particles.

$$3Al_2O_3{\cdot}2SiO_2 \rightarrow 3Al_2O_3 + 2SiO_2, \quad (1)$$

$$Al_2O_3 + ZnO \rightarrow ZnAl_2O_4, \quad (2)$$

$$SiO_2 + ZnO \rightarrow Zn_2SiO_4 \quad (3)$$

At the same time, it can be shown from Fig. 4 that the ZnO peaks become higher while the intensity of the $3Al_2O_3{\cdot}2SiO_2$, $ZnAl_2O_4$ and Zn_2SiO_4 peaks reduces slightly with increasing ZnO content on the whole. When the ZnO content is 80 wt.%, $3Al_2O_3{\cdot}2SiO_2$ peak is weak. This result reveals that most of mullite has completely decomposed and reacted with ZnO, resulting in more ZnO remained in the coatings.

As dielectric properties of ZnO/mullite coating are very sensitive to ZnO content in the coatings, we measured the XRD patterns of coatings with different ZnO content annealed at

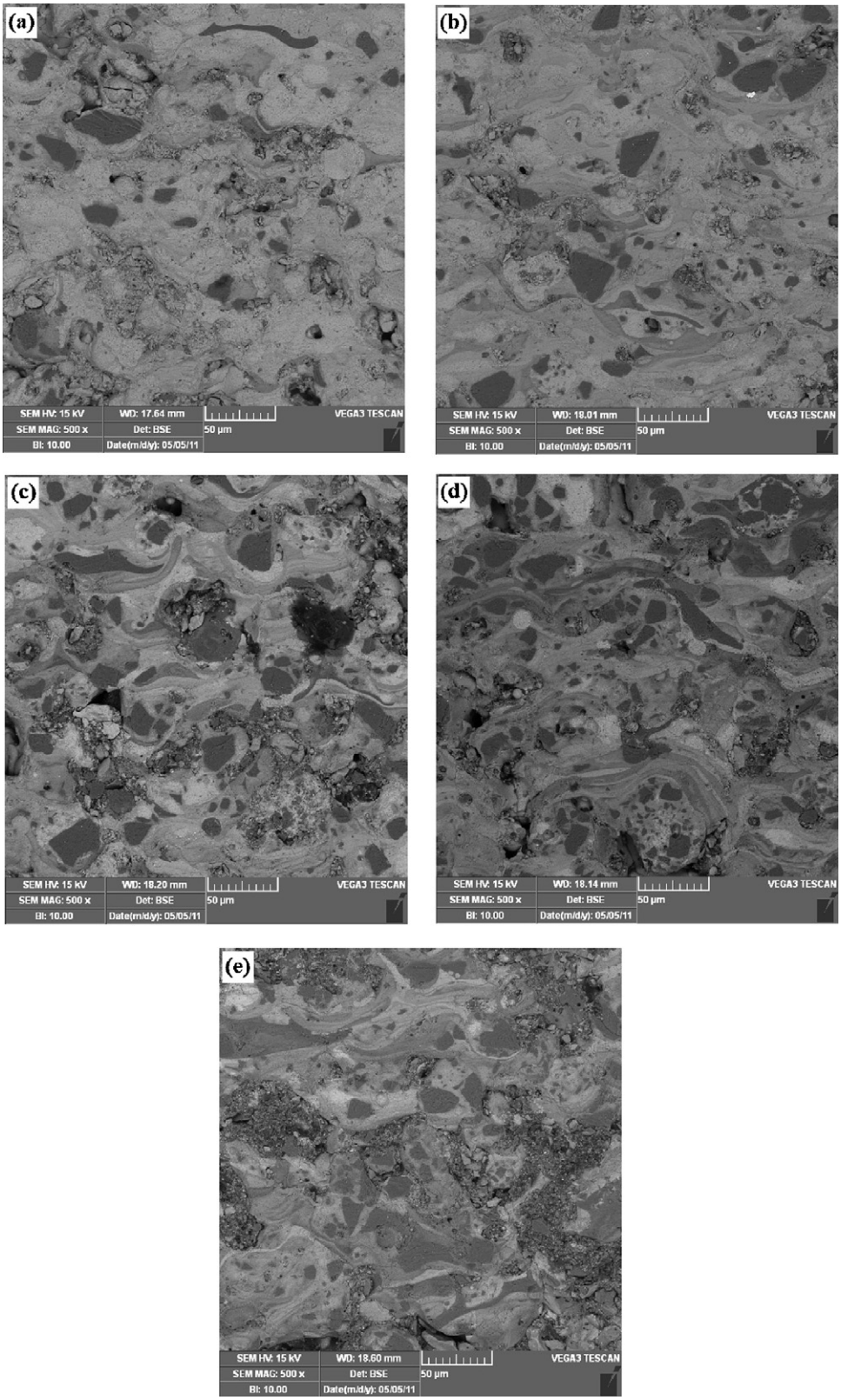

Fig. 3. Cross-sectional SEM morphologies of the as-sprayed ZnO/mullite composite coating with different ZnO content: (a) 40 wt.% ZnO; (b) 50 wt.% ZnO; (c) 60 wt.% ZnO; (d) 70 wt.% ZnO; (e) 80 wt.% ZnO.

900 °C for 5 h. From the XRD patterns of the annealed coatings shown in Fig. 5, we can observe that all the samples contain ZnO, $3Al_2O_3{\cdot}2SiO_2$, $ZnAl_2O_4$ and Zn_2SiO_4. Furthermore, as the ZnO content increases from 40 wt.% to 80 wt.%, the intensity of ZnO diffraction peaks increases while those of $3Al_2O_3{\cdot}2SiO_2$, $ZnAl_2O_4$ and Zn_2SiO_4 decrease dramatically. Furthermore, the coatings after annealed show more $3Al_2O_3{\cdot}2SiO_2$, $ZnAl_2O_4$, Zn_2SiO_4 phases and less ZnO phase

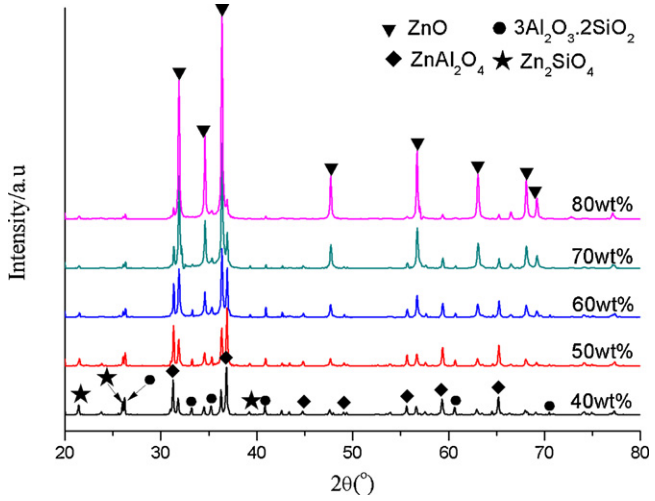

Fig. 4. X-ray diffraction of the as-sprayed ZnO/mullite composite coatings.

compared with as-sprayed coatings as shown in Figs. 4 and 5. This result indicates that more chemical reactions have been conducted after the annealing at 900 °C which leads to the decrease of ZnO content in the composite coatings.

3.3. Dielectric properties of coatings

3.3.1. Effect of ZnO content on dielectric properties

Fig. 6 illustrates the real (ε') and the imaginary (ε'') part of the dielectric constant in the frequency range of 8.2–12.4 GHz for the ZnO/mullite composite coatings. Both the real part and imaginary part increase with the ZnO content increased from 40 wt.% to 80 wt.%, while the rapid increase in ε' and ε'' could be seen in the composite coatings with 60, 70 and 80 wt.%. We ascribe this rapid increase to the formation of the ZnO local network as shown in Fig. 3. The possibility of contact between ZnO splats increases as the proportion of ZnO increases, thus ZnO networks form readily at higher ZnO contents. Such phenomenon has already been found by various authors [20–22]. It also can be seen that, the real part of the coatings with lower ZnO content (40, 50 and 60 wt. %) remain almost constant in the whole frequency range, while the real part of coatings with higher ZnO content tended to decrease with increasing frequency and represented frequency dependence in the whole frequency range.

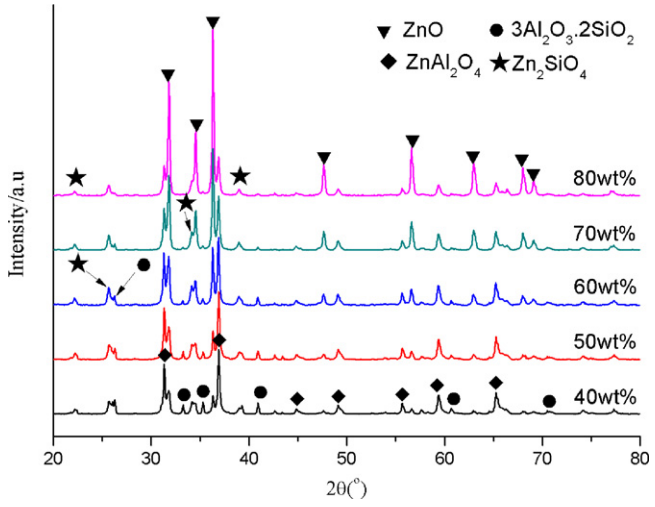

Fig. 5. X-ray diffraction of the annealed ZnO/mullite composite coatings.

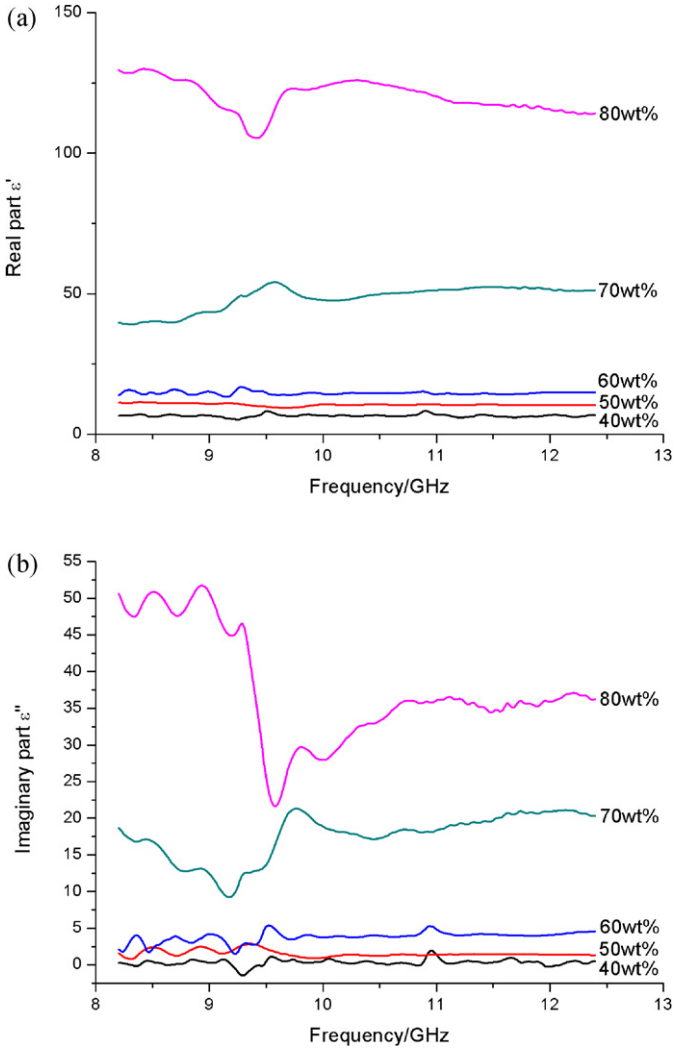

Fig. 6. (a) The real part (ε') and (b) the imaginary part (ε'') of as-sprayed coatings versus frequency.

For the heterogeneous system of ZnO/mullite composite coatings, the properties of interfaces could have a dominant role in determining dielectric performance, and interfacial polarization induced by the charge along the boundaries of ZnO splats is an important polarization process and associated relaxation also gives rise to loss mechanism. On the other hand, it has been shown in our previous paper [23] that ZnO is a polar semiconductor. Orientation polarization is an important polarization and associated relaxation will give rise to dielectric loss mechanism of ZnO/mullite composite coatings. Composite coatings, in which dielectric ZnO particles impinged in the $3Al_2O_3{\cdot}2SiO_2$, $ZnAl_2O_4$ and Zn_2SiO_4 composite, additional dielectric interfaces, and more polarization charges on the surface of ZnO particles make the behaviors of dielectric relaxation more complex. Thus, it is considered that orientation polarization and interfacial polarization play roles in the complex permittivity of such composite coatings. It is reasonable that the higher ε' and ε''' values can be obtained when the composite coatings are filled

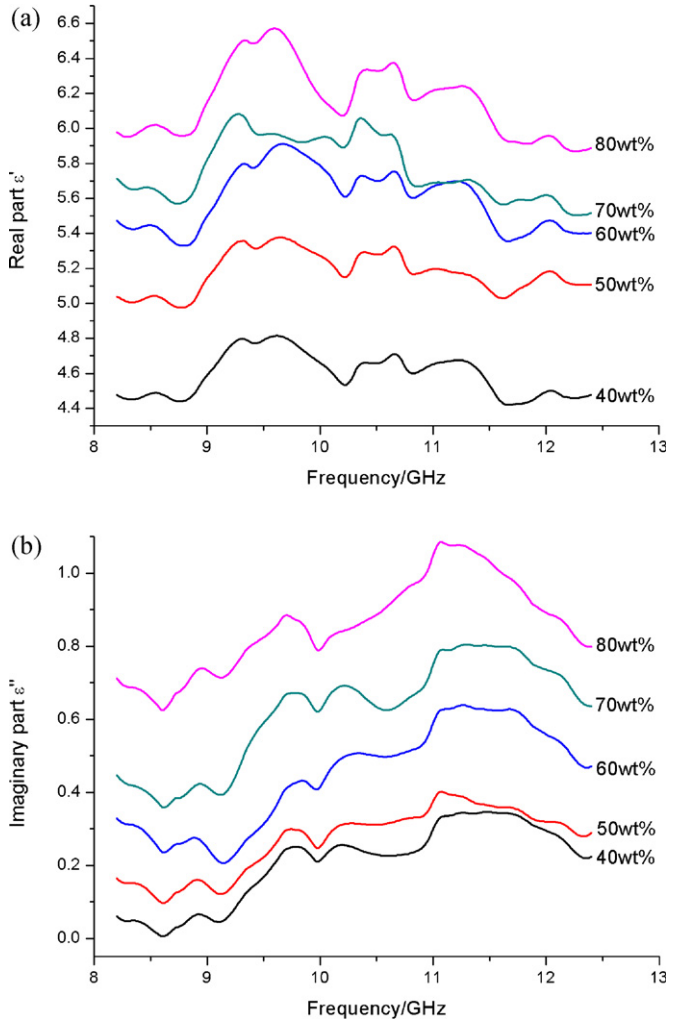

Fig. 7. (a) The real part (ε') and (b) the imaginary part (ε'') of annealed coatings versus frequency.

with a higher ZnO content, due to the higher orientation polarization and relaxation polarization of ZnO constituent.

3.3.2. *Effect of annealing on dielectric properties*

In order to investigate the high-temperature microwave absorption properties, we make the as-sprayed coating annealed under 900 °C for 5 h. Fig. 7 shows the complex permittivity of ZnO/mullite composite coatings annealed under 900 °C for 5 h. Both ε' and ε'' apparently increase with increasing ZnO content, which represents the same trend with the as-sprayed coating. Compared with the as-sprayed coatings, both ε' and ε'' decrease greatly after annealed under 900 °C as illustrated in Fig. 7. It is proposed that further reactions between ZnO and mullite have been conducted in high temperature which result in more $ZnAl_2O_4$, Zn_2SiO_4 phases and less ZnO remained in the composite coatings as shown in Figs. 4 and 5. According to the effective medium theory [24,25], the complex permittivity decreases with the concentration of conductive particles decreasing. In addition, the decrease in the number of continuous conductive ZnO particles in the composite coatings would also lead to weaken electrical conductivity, contributing to the decreased dielectric loss of the coatings after annealed in high temperature.

4. Conclusions

The ZnO/mullite composite absorber coatings were fabricated by atmosphere plasma spraying (APS) technique. The microstructure and crystalline phase of coatings were studied. The coatings show a dense structure with a few pores, and ZnO particles impinge on the $ZnAl_2O_4$, Zn_2SiO_4 and mullite matrix. The dielectric properties of coatings with different ZnO content were studied in detail in a frequency range of 8.2–12.4 GHz. The coatings with higher ZnO content present higher dielectric real part (ε') and imaginary part (ε''), which are ascribed to interfacial polarization and orientation polarization. In addition, coatings after annealed under high temperature represent much lower complex permittivity compared with the as-sprayed coatings, which is induced by further reactions between ZnO and mullite. Therefore, optimizing the dielectric properties through ZnO content and annealing temperature, ZnO/mullite composite coatings are potentially employed in wave-absorbing field.

Acknowledgement

This work was supported by National Natural Science Foundation of China (No. 51072165).

References

[1] P. Fauchais, Understanding plasma spraying, J. Phys. D: Appl. Phys. 37 (2004) 86–108.
[2] J. Anggono, B. Derby, Pyrolysis of aluminium loaded polymethylsiloxanes: the influence of Al/PMS ratio on mullite formation, J. Mater. Sci. 45 (2010) 233–241.
[3] A. Priya, S. Nath, K. Biswas, et al., In vitro dissolution of calcium phosphate-mullite composite in simulated body fluid, J. Mater. Sci. 21 (2010) 1817–1828.
[4] K.K. Chawla, Interface engineering in mullite fiber/mullite matrix composites, J. Eur. Ceram. Soc. 28 (2008) 447–453.
[5] G. Di Girolamo, C. Blasi, L. Pilloni, et al., Microstructural and thermal properties of plasma sprayed mullite coatings, Ceram. Int. 36 (2010) 1389–1395.
[6] S. Seifert, E. Litovsky, J.I. Kleiman, et al., Thermal resistance and apparent thermal conductivity of thin plasma-sprayed mullite coatings, Surf. Coat. Technol. 200 (2006) 3404–3410.
[7] C. Cano, E. Garcia, A.L. Fernandes, et al., Mullite/ZrO_2 coatings produced by flame spraying, J. Eur. Ceram. Soc. 28 (2008) 2191–2197.
[8] S. Rangaraj, K. Kokini, Interface thermal fracture in functionally graded zirconia–mullite–bond coat alloy thermal barrier coatings, Acta Mater. 51 (2003) 251–267.
[9] C. Aksel, The effect of mullite on the mechanical properties and thermal shock behaviour of alumina–mullite refractory materials, Ceram. Int. 29 (2003) 183–188.
[10] H.R. Rezaie, W.M. Rainforth, W.E. Lee, Fabrication and Mechanical Properties of SiC Platelet Reinforced Mullite Matrix Composites, J. Eur. Ceram. Soc. 19 (1999) 1777–1787.
[11] J.S. Moya, M. Díaz, C.F. Gutiérrez-González, et al., Mullite-refractory metal (Mo, Nb) composites, J. Eur. Ceram. Soc. 28 (2008) 479–491.
[12] J. Huo, L. Wang, H. Yu, Polymeric nanocomposites for electromagnetic wave absorption, J. Mater. Sci. 44 (2009) 3917–3927.
[13] A. Gupta, V. Choudhary, Electrical conductivity and shielding effectiveness of poly(trimethylene terephthalate)/multiwalled carbon nanotube composites, J. Mater. Sci. 46 (2011) 6416–6423.
[14] Oku, Mitsumasa, European Patent, Patent Application Number: 92103630.7.

[15] Z. Dang, L. Fan, S. Zhao, et al., Dielectric properties and morphologies of composites filled with whisker and nanosized zinc oxide, Mater. Res. Bull. 38 (2003) 499–507.
[16] Y.C. Qing, W.C. Zhou, F. Luo, et al., Microwave electromagnetic properties of carbonyl iron particles and Si/C/N nano-powder filled epoxy-silicone coating, Phys. B 405 (2010) 1181–1184.
[17] N.Q. Zhao, T.C. Zou, C.S. Shi, et al., Microwave absorbing properties of activated carbon-fiber felt screens (vertical-arranged carbon fibers)/epoxy resin composites, Mater. Sci. Eng. B 127 (2006) 207.
[18] H. Mahdjoub, P. Roy, C. Filiatre, et al., The effect of the slurry formulation upon the morphology of spray-dried yttria stabilised zirconia particles, J. Eur. Ceram. Soc. 23 (2003) 1637–1648.
[19] E.N. Bunting, Res. J Nall. Stand. Bur. 8 (2) (1932) 286, RP413.
[20] M.S. Cao, X.L. Shi, X.Y. Fang, et al., Microwave absorption properties and mechanism of cagelike ZnO/SiO_2 nanocomposites, Appl. Phys. Lett. 91 (2007) 203110.
[21] H. Zois, L. Apekis, Y.P. Mamunya, Dielectric properties and morphology of polymer composites filled with dispersed iron, J. Appl. Polym. Sci. 88 (2003) 3013–3020.
[22] V. Singh, A.R. Kulkarni, T.R. Rama Mohan, Dielectric properties of aluminum-epoxy composites, J. Appl. Polym. Sci. 90 (2003) 3602–3608.
[23] L. Zhou, W. Zhou, T. Liu, et al., Influence of ZnO content and annealing temperature on the dielectric properties of ZnO/Al_2O_3 composite coatings, J. Alloys Compd. 509 (2011) 5903–5907.
[24] L. Wang, Z.M. Dang, Carbon nanotube composites with high dielectric constant at low percolation threshold, Appl. Phys. Lett. 87 (2005) 042903.
[25] W.L. Song, M.S. Cao, Z. Hou, et al., High-temperature microwave absorption and evolutionary behavior of multiwalled carbon nanotube nanacomposite, Scripta Mater. 61 (2009) 201–204.